Chapter 3

Lecture 9

Drag polar – 4

Topics

3.2.11 Presentation of aerodynamic characteristics of airfoils
3.2.12 Geometric characteristics of airfoils
3.2.13 Airfoil nomenclature\designation
3.2.14 Induced drag of wing
3.2.15 Drag coefficient of fuselage
3.2.16 Drag coefficients of other components
3.2.17 Parabolic drag polar, parasite drag, induced drag and Oswald efficiency factor

3.2.11. Presentation of aerodynamic characteristics of airfoils

As mentioned in the beginning of subsection 3.2.3, the ways of presenting the aerodynamic and geometric characteristics of the airfoils and the nomenclature of the airfoils are discussed in this and the next two subsections.

Figure 3.18 shows typical experimental characteristics of an aerofoil. The features of the three plots in this figure can be briefly described as follows.

(I) Lift coefficient (C_l) vs angle of attack (α). This curve, shown in Fig.3.18a, has four important features viz. (a) angle of zero lift (α_{0l}), (b) slope of the lift curve denoted by $dC_l / d\alpha$ or a_0 or $C_{l\alpha}$, (c) maximum lift coefficient ($C_{l\max}$) and (d) angle of attack (α_{stall}) corresponding to $C_{l\max}$.

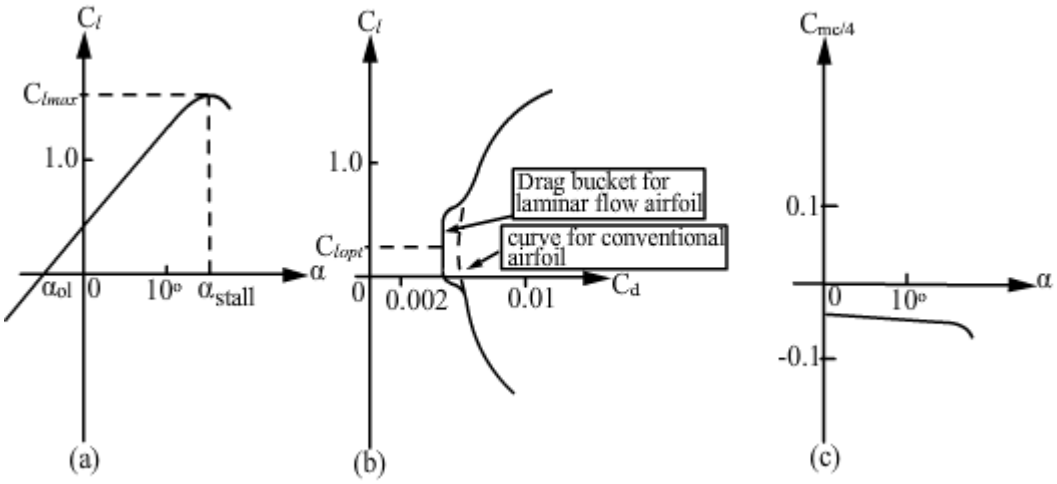

Fig.3.18 Aerodynamic characteristics of an airfoil

(a) C_l vs α (b) C_l vs C_d (c) $C_{mc/4}$ vs α

(II) Drag coefficient (C_d) vs C_l. This curve, shown in Fig.3.18b, has two important features viz. (a) minimum drag coefficient (C_{dmin}) and (b) lift coefficient (C_{lopt}) corresponding to C_{dmin}. In some airfoils, called laminar flow airfoils or low-drag airfoils, the minimum drag coefficient extends over a range of lift coefficients (Fig.3.18b). This feature is called 'Drag bucket'. The extent of the drag bucket and the lift coefficient at the middle of this region are also characteristic features of the airfoil. It may be added that the camber decides C_{lopt} and thickness ratio decides the extent of the drag bucket.

(III) Pitching moment coefficient about quarter-chord $C_{mc/4}$ vs α . This curve is shown in Fig.3.18c. Sometimes this curve is also plotted as $C_{mc/4}$ vs C_l. From this curve, the location of the aerodynamic center (a.c.) and the moment about it (C_{mac}) can be worked out. It may be recalled that a.c. is the point on the chord about which the moment coefficient is independent of C_l.

(IV) Stall pattern : Variation of the lift coefficient with angle of attack near the stall is an indication of the stall pattern. A gradual pattern as shown in Fig.3.18a is a desirable feature. Some airfoils display abrupt decrease in C_l after stall. This behaviour is undesirable as pilot does not get adequate warning regarding

impending loss of lift. Airfoils with thickness ratio between 6 – 10% generally display abrupt stall while those with t/c more than 14% display a gradual stall. It may be added that the stall patterns on the wing and on the airfoil are directly related only for high aspect ratio (A > 6) unswept wings. For low aspect ratio highly swept wings three-dimensional effects may dominate.

3.2.12 Geometrical characteristics of airfoils

To describe the geometrical characteristics of airfoils, the procedure given in chapter 6 of Ref.3.14 is followed. In this procedure, the camber line or the mean line is the basic line for definition of the aerofoil shape (Fig.3.19a). The line joining the extremities of the camber line is the chord. The leading and trailing edges are defined as the forward and rearward extremities, respectively, of the mean line. Various camber line shapes have been suggested and they characterize various families of airfoils. The maximum camber as a fraction of the chord length (y_{cmax}/c) and its location as a fraction of chord (x_{ycmax}/c) are the important parameters of the camber line.

Various thickness distributions have been suggested and they characterize different families of airfoils Fig.3.19b. The maximum ordinate of the thickness distribution as fraction of chord (y_{tmax}/c) and its location as fraction of chord (x_{ytmax}/c) are the important parameters of the thickness distribution.

Airfoil shape and ordinates:

The aerofoil shape (Fig.3.19c) is obtained by combining the camber line and the thickness distribution in the following manner.

a) Draw the camber line shape and draw lines perpendicular to it at various locations along the chord (Fig.3.19c).

b) Lay off the thickness distribution along the lines drawn perpendicular to the mean line (Fig.3.19c).

c) The coordinates of the upper surface (x_u, y_u) and lower surface (x_l, y_l) of the airfoil are given as :

$$\left.\begin{aligned} x_u &= x - y_t \sin\theta \\ y_u &= y_c + y_t \cos\theta \\ x_l &= x + y_t \sin\theta \\ y_l &= y_c - y_t \cos\theta \end{aligned}\right\} \quad \text{----------} \quad (3.37)$$

where y_C and y_t are the ordinates, at location x, of the camber line and the thickness distribution respectively; tan θ is the slope of the camber line at location x (see also Fig.3.19d).

d) The leading edge radius is also prescribed for the aerofoil. The center of the leading edge radius is located along the tangent to the mean line at the leading edge (Fig.3.19c).

e) Depending on the thickness distribution, the trailing edge angle may be zero or have a finite value. In some cases, thickness may be non-zero at the trailing edge.

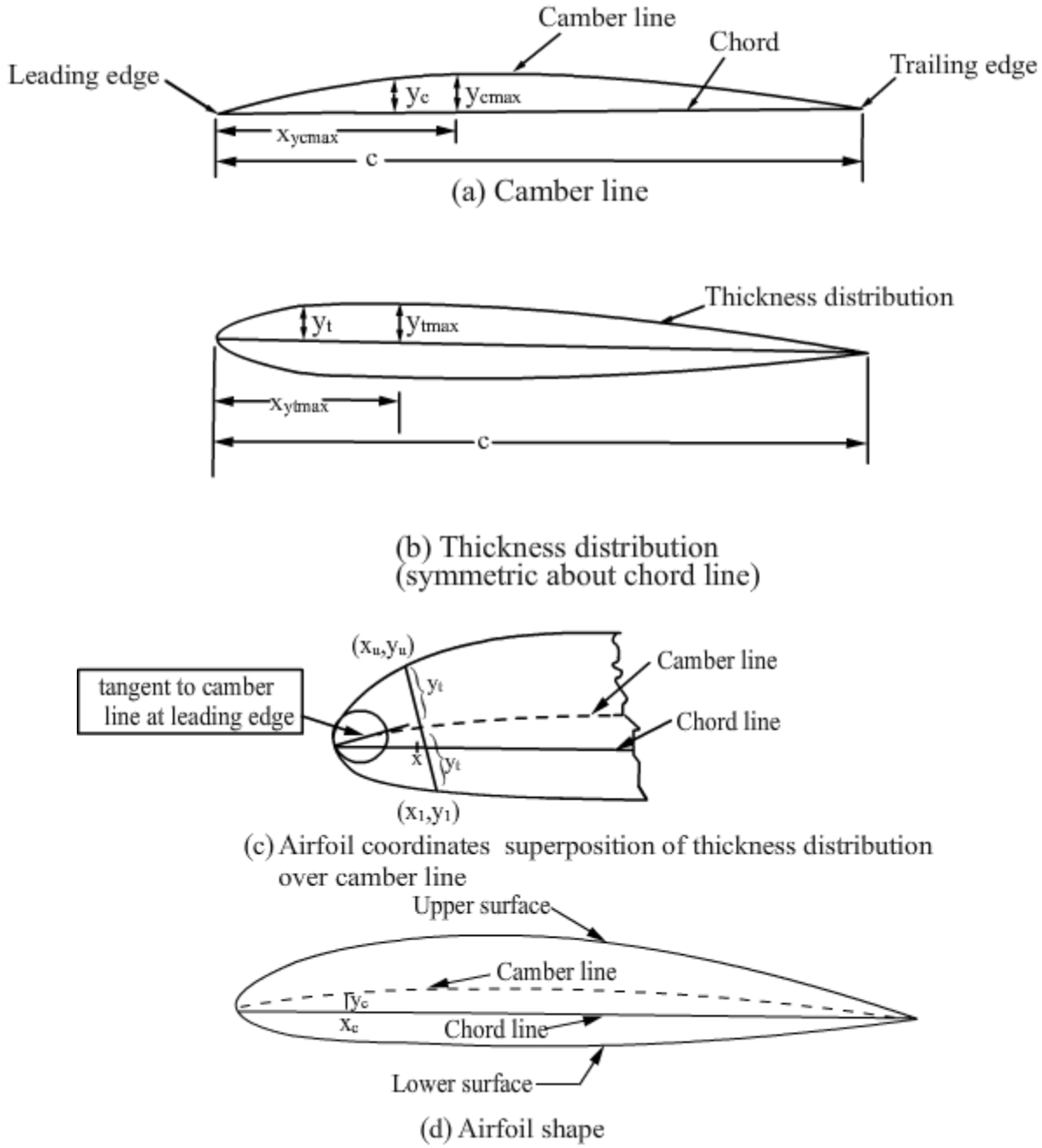

Fig.3.19 Airfoil geometry

3.2.13 Airfoil nomenclature/designation

Early airfoils were designed by trial and error. Royal Aircraft Establishment (RAE), UK and Gottingen laboratory of German establishment which is now called DLR(Deutsches Zentrum für Luft-und Raumfahrt – German

Centre for Aviation and Space Flight) were pioneers in airfoil design. Clark Y airfoil shown in Fig.3.20a is an example of a 12% thick airfoil with almost flat bottom surface which has been used on propeller blades.

Taking advantage of the developments in airfoil theory and boundary layer theory, NACA (National Advisory Committee for Aeronautics) of USA systematically designed and tested a large number of airfoils in 1930's. These are designated as NACA airfoils. In 1958 NACA was superseded by NASA (National Aeronautic and Space Administration). This organization has developed airfoils for special purposes. These are designated as NASA airfoils. Though the large airplane companies like Boeing and Airbus, design their own airfoils the NACA and NASA airfoils are generally employed by others. A brief description of their nomenclature is presented below. The description of NACA airfoils is based on chapter 6 of Ref.3.14.

NACA four-digit series airfoils

Earliest NACA airfoils were designated as four-digit series. The thickness distribution was based on successful RAE & Gottigen airfoils. It is given as :

$$\pm y_t = \frac{t}{20}\left[0.2969\sqrt{x} - 0.1260\,x - 0.3516\,x^2 + 0.2843\,x^3 - 0.1015\,x^4\right] \qquad (3.38)$$

where t = maximum thickness as fraction of chord.

The leading radius is : $r_t = 1.1019\ t^2$

Appendix I of Ref.3.14 contains ordinates for thickness ratios of 6%, 9%, 10%, 12%, 15%, 18%, 21% and 24%. The thickness distributions are denoted as NACA 0006, NACA 0009,……..,NACA 0024. Figure 3.20b shows the shape of NACA 0009 airfoil. It is a symmetrical airfoil by design. The maximum thickness of all four-digit airfoils occurs at 30% of chord. In the designation of these airfoils the first two digits indicate that the camber is zero and the last two digits indicate the thickness ratio as percentage of chord.

a) Clark Y – Airfoil with flat bottom surface, used on propeller blades

b) NACA 0009 – Symmetrical airfoil used on control surfaces

c) NACA 23012 – Airfoil with high C_{lmax} , used on low speed airplanes

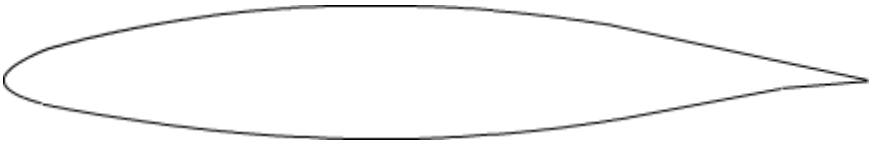

d) NACA 66_2 – 215 – Laminar flow or low drag airfoil

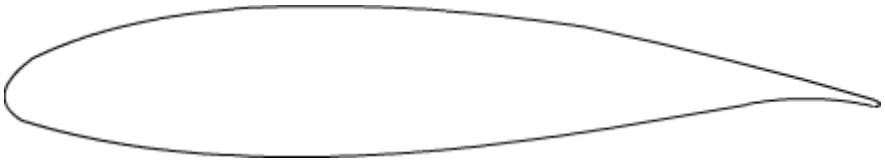

e) NASA GA(W) -1 or LS(1) - 0417 – Airfoil specially designed for general aviation airplanes

f) NASA SC(2)-0714 – Supercritical airfoil with high critical Mach number, specially designed for high subsonic airplanes

Fig.3.20 Typical airfoils

The camber line for the four-digit series airfoils consists of two parabolic arcs tangent at the point of maximum ordinate. The expressions for camber(y_c) are :

$$\left.\begin{aligned} y_c &= \frac{m}{p^2}\left(2px - x^2\right);\ x \le x_{ycmax} \\ &= \frac{m}{(1-p)^2}\left[(1-2p) + 2px - x^2\right];\ x > x_{ycmax} \end{aligned}\right\} \qquad (3.39)$$

m = maximum ordinate of camber line as fraction of chord

p = chordwise position of maximum camber as fraction of chord

The camber lines obtained by using different values of m & p are denoted by two digits, e.g. NACA 64 indicates a mean line of 6% camber with maximum camber occuring at 40% of the chord. Appendix II of Ref.3.14 gives ordinates for NACA 61 to NACA 67 mean lines. The ordinates of other meanlines are obtained by suitable scaling. For example, NACA 24 mean lines is obtained by multiplying the ordinates of NACA 64 mean line by (2/6).

A cambered airfoil of four-digit series is obtained by combining meanline and the thickness distribution as described in the previous subsection. For example, NACA 2412 airfoil is obtained by combining NACA 24 meanline and NACA 0012 thickness distribution. This airfoil has (a) maximum camber of 2% occurring at 40% chord and (b) maximum thickness ratio of 12%.

Refer appendix III of Ref.3.14, for ordinates of the upper and lower surfaces of several four-digit series airfoils. Appendix IV of the same reference presents the low speed aerodynamic characteristics at M = 0.17 and various Reynolds numbers. Chapter 7 of the same reference gives details of experimental conditions and comments on the effects of parameters like camber, thickness ratio, Reynolds number and roughness on aerodynamic characteristics of airfoils.

NACA five-digit series airfoils

During certain tests it was observed that $C_{l_{max}}$ of the airfoil could be increased by shifting forward the location of the maximum camber. This finding led to development of five-digit series airfoils. The new camber lines for the five-digit series airfoils are designated by three digits. The same thickness distribution

was retained as that for NACA four-digit series airfoils. The camber line shape is given as :

$$\left.\begin{aligned} y_c &= \frac{1}{6}k_1\left[x^3 - 3mx^2 + m^2(3-m)x\right],\ 0 < x \le m \\ &= \frac{1}{6}k_1 m^3\left[1-x\right];\ m < x < 1 \end{aligned}\right\} \text{----------(3.40)}$$

The value of 'm' decides the location of the maximum camber and that of k_1 the design lift coefficient(C_{li} or $C_{l_{opt}}$). A combination of m = 0.2025 and k_1 = 15.957 gives C_{li} = 0.3 and maximum camber at 15% of chord. This meanline is designated as NACA 230. The first digit '2' indicates that C_{li} = 0.3 and the subsequent two digits (30) indicate that the maximum camber occurs at 15% of chord.

A typical five-digit cambered airfoil is NACA 23012. Its shape is shown in Fig.3.20c. The digits signify :

First digit(2) indicates that C_{li} = 0.3.

Second & third digits (30) indicate that maximum camber occurs at 15% of chord.

Last two digits (12) indicate that the maximum thickness ratio is 12%.

Remarks:

(i) Refer Appendices II, III and IV of Ref.3.14 for camber line shape, ordinates and aerodynamic characteristics of five-digit series airfoils.

(ii) Modified four and five digit series airfoils were obtained when leading edge radius and position of maximum thickness were altered. For details Ref.3.14, chapter 6 may be consulted.

Six series airfoils

As a background to the development of these airfoils the following points may be mentioned.

(i) In 1931 T.Theodorsen presented 'Theory of wing sections of arbitrary shape' NACA TR 411 which enabled calculation flow past airfoils of general shape .

(ii) Around the same time the studies of Tollmien and Schlichting on boundary layer transition, indicated that the transition process, which causes laminar boundary layer to become turbulent, depends predominantly on the pressure gradient in the flow around the airfoil.

(iii) A turbulent boundary layer results in a higher skin friction drag coefficient as compared to when the boundary layer is laminar. Hence, maintaining a laminar boundary layer over a longer portion of the airfoil would result in a lower drag coefficient.

(iv) Inverse methods, which could permit design of meanline shapes and thickness distributions, for prescribed pressure distributions were also available.

Taking advantage of these developments, new series of airfoils called low drag airfoils or laminar flow airfoils were designed. These airfoils are designated as 1-series, 2-series,……..,7-series. Among these the six series airfoils are commonly used airfoils. Refer Ref.3.14, chapter 6 for more details.

When the airfoil surface is smooth. These airfoils have a C_{dmin} which is lower than that for four-and five-digit series airfoils of the same thickness ratio. Further, the minimum drag coefficient extends over a range of lift coefficient. This extent is called drag bucket (see Fig.3.18b).

The thickness distributions for these airfoils are obtained by calculations which give a desired pressure distribution. Analytical expressions for these distributions are not available. Appendix I of Ref.3.14 gives symmetrical thickness distributions for t/c between 6 to 21%.

The camber lines are designated as : a = 0, 0.1, 0.2 …., 0.9 and 1.0. For example, the camber line shape with a = 0.4 gives a uniform pressure distribution from x/c = 0 to 0.4 and then linearly decreasing to zero at x/c = 1.0. If the camber line designation is not mentioned, 'a' equal to unity is implied.

An airfoil with a designation as NACA 66_2-215 is shown in Fig.3.20d. It is obtained by combining NACA 66_2 – 015 thickness distribution and a = 1.0 mean line. The digits signify :

1st digit '6' indicates that it is a 6 series airfoil

2nd digit '6' denotes the chordwise position of the minimum pressure in tenths of chord for the symmetrical airfoil at $C_l = 0$. i.e. the symmetrical section

(NACA 66_2 - 015) would have the minimum pressure at x/c = 0.6 when producing zero lift.

The suffix '2' indicates that the drag bucket extends ± 0.2 around $C_{l_{opt}}$.

The digit '2' after the dash indicates that $C_{l_{opt}}$ is 0.2. Thus in this case, drag bucket extends for C_l = 0.0 to 0.4.

The last two digits "15" indicate that the thickness ratio is 15%.

Since the value of 'a' is not explicitly mentioned, the camber line shape corresponds to a = 1.0.

Remarks:

(i) Refer appendices I, II, III and IV of Ref.3.14 for details of thickness distribution, camber distribution, ordinates and aerodynamic characteristics of various six series airfoils.

(ii) The lift coefficient at the centre of the drag bucket ($C_{l_{opt}}$) depends on the camber. The extent of drag bucket depends on the thickness ratio and the Reynolds number. The value given in the designation of the airfoil is at $R_e = 9 \times 10^6$. The extent is about ± 0.1 for t/c of 12%, ± 0.2 for t/c of 15% and ± 0.3 for t/c of 18%. When the extent of the drag bucket is less than ± 0.1, the subscript in the designation of the airfoil is omitted, e.g. NACA 66-210

NASA airfoils

NASA has developed airfoil shapes for special applications. For example GA(W) series airfoils were designed for general aviation airplanes. The 'LS' series of airfoils among these are for low speed airplanes. A typical airfoil of

this category is designated as LS(1)-0417. In this designation, the digit '1' refers to first series, the digits '04' indicate $C_{l_{opt}}$ of 0.4 and the digits '17' indicate the thickness ratio of 17%. Figure 3.20c shows the shape of this airfoil. For the airfoils in this series, specifically designed for medium speed airplanes, the letters 'LS' are replaced by 'MS'.

NASA NLF series airfoils are 'Natural Laminar Flow' airfoils.

NASA SC series airfoils are called 'Supercritical airfoils'. These airfoils have a higher critical Mach number. Figure 3.20f shows an airfoil of this category. Chapter 3 of Ref.1.9 may be referred to for further details.

Remarks:

(i)Besides NACA & NASA airfoils, some researchers have designed airfoils for specialized applications like (a) low Reynolds number airfoils for micro air vehicles, (b) wind mills, (c) hydrofoils etc. These include those by Lissaman, Liebeck, Eppler and Drela. Reference 3.9, chapter 4, and internet (www.google.com) may be consulted for details.

(ii)The coordinates of NACA, NASA and many other airfoils are available on the website entitled 'UIUC airfoil data base'.

3.2.14 Induced drag of wing

In the beginning of section 3.2.2 it was mentioned that the drag of the wing consists of (i) the profile drag coefficient due to airfoil (C_d) and (ii) the induced drag coefficient (C_{Di}) due to finite aspect ratio of the wing. Subsections 3.2.3 to 3.2.13 covered various aspects of profile drag. In this subsection the induced drag of the wing is briefly discussed.

For details regarding the production of induced drag and derivation of the expression for the induced drag coefficient, the books on aerodynamics can be consulted e.g. Ref.3.12, chapter 5. Following is a brief description of the induced drag.

Consider a wing kept at a positive angle of attack in an air stream. In this configuration, the wing produces a positive lift. At the wing root, the average pressure on the upper surface is lower than the free stream pressure (p_∞) and

the average pressure on the lower surface is higher than p_∞. Since the span of the wing is finite it has the wing tips and at these tips there cannot be a pressure discontinuity or the pressure at the wing tips would be the same on the upper side and the lower side. The pressure at the wing tips is expected to be mean of the pressures on the upper and lower sides at the root section. Because of the difference of pressures between the root and the tip, the pressure on the upper surface of the wing increases from root to the tip in the spanwise direction. Similarly, the pressure on the lower surface of the wing, decreases from the root to the tip in the spanwise direction. These pressure gradients on the upper and lower surfaces would lead to cross flows on these surfaces. Thus, at a given spanwise station, the airstreams from the upper and lower surfaces would meet, at the trailing edge, at an angle. This would cause shedding of vortices from the trailing edge. Viewed from the rear, the vortices would appear rotating clockwise from the left wing and anticlockwise from the right wing. These vortices soon roll up to form two large vortices springing from positions near the wing tips. As a consequence of these vortices the air stream in the vicinity and behind the wing acquires a downward velocity component called induced downwash.
This downwash tilts the aerodynamic force rearwards resulting in a component in the free stream direction called induced drag. The induced drag coefficient (C_{Di}) is given as :

$$C_{Di} = \frac{C_L^2(1+\delta)}{\pi A} = \frac{C_L^2}{\pi A e_{wing}} \qquad (3.41)$$

Where A is the wing aspect ratio ($A = b^2/S$) and δ is a factor which depends on wing aspect ratio, taper ratio, sweep and Mach number. The quantity 'e_{wing}' is called Oswald efficiency factor for wing.

It may be added that a wing with elliptic chord distribution has the minimum induced drag i.e. $\delta = 0$ in Eq.(3.41).

Reference 3.6 section 3.3, gives the following expression for e_{wing} which is based on Ref.3.5 section 4.1.5.2.

$$e_{wing} = \frac{1.1\left(C_{L\alpha W}/A\right)}{R\left(\frac{C_{L\alpha W}}{A}\right)+(1-R)\pi} \qquad (3.42)$$

where,

$$C_{L\alpha W} = \frac{2\pi A}{2+\sqrt{\frac{A^2\beta^2}{\kappa^2}\left(1+\frac{\tan^2\Lambda_{\frac{1}{2}}}{\beta^2}\right)+4}} \qquad (3.43)$$

$C_{L\alpha W}$ = slope of lift curve of wing in radians

A = aspect ratio of wing

R = a factor which depends on (a) Reynolds number based on leading edge radius, (b) leading edge sweep (Λ_{LE}), (c) Mach number (M), (d) wing aspect ratio (A) and (e) taper ratio (λ).

$\beta = \sqrt{1-M^2}$

$\Lambda_{1/2}$ = sweep of semi-chord line

κ = ratio of the slope of lift curve of the airfoil used on wing divided by 2π. It is generally taken as unity.

Remarks:

(i)Example 3.3 illustrates the estimation of e_{wing} for an unswept wing. Section 2.5 of Appendix 'B' illustrates the steps for estimating e_{wing} of a jet airplane.

(ii) When a flap is deflected, there will be increments in lift coefficient and also in profile drag coefficient and induced drag coefficient. Refer section 2.9 of Appendix 'A'.

(iii) The drags of horizontal and vertical tails, can be estimated by following a procedure similar to that for the wing. However, contributions to induced drag from the tail surfaces are generally neglected.

3.2.15 Drag coefficient of fuselage

The drag coefficient of a fuselage (C_{Df}) consists of (a)the drag of the fuselage at zero angle of attack $(C_{Do})_f$ plus (b) the drag due to angle of attack. Following

Ref.3.7, section 19.3 it can be expressed as:

$$C_{Df} = C_{Dof}\left\{1+K\left(\frac{\alpha}{15}\right)^2\right\} \qquad (3.44)$$

where α is the angle of attack of fuselage in degrees.

For a streamlined body $(C_{Do})_f$ is mainly skin friction drag and depends on (i) Reynolds number, based on length of fuselage (l_f), (ii) surface roughness and (iii) fineness ratio (A_f). The fineness ratio is defined as:

$$A_f = l_f / d_e \qquad (3.44a)$$

'd_e' is the equivalent diameter given by:

$$(\pi/4)d_e^2 = A_{fmax}$$

where A_{fmax} equals the area of the maximum cross-section of the fuselage.

When the fineness ratio of the fuselage is small, for example, in case of general aviation airplanes, the fuselage may be treated as a bluff body. In such a case the term C_{Dof} is mainly pressure drag and the drag coefficient is based on the frontal area (A_{fmax}). However, the expression for $(C_{D0})_f$ given in Ref.3.6, section 3.1.1 includes the effect of pressure drag and is also valid for general aviation airplanes (refer section 2 of Appendix A).

The quantity 'K' in Eq.(3.44) has a value of 1 for a circular fuselage and 4 to 6 for a rectangular fuselage. However, the general practice is to include the increase in drag of fuselage, due to angle of attack, by adding a term $\left(\frac{1}{e_{fuselage}}\right)$ to $\left(\frac{1}{e_{wing}}\right)$.

Remark:

The drag coefficients of other bodies like engine nacelle, external fuel tanks and bombs suspended from the wing, can also be estimated in a manner similar to that of fuselage.

3.2.16 Drag coefficients of other components

The drag coefficients of other components like landing gear are based on areas specific to those components. They should be obtained from the sources of drag data mentioned earlier. The change in drag of these components, with angle of attack, is included by adding a term $\left(\frac{1}{e_{other}}\right)$ to $(\frac{1}{e_{fuselage}} + \frac{1}{e_{wing}})$ i.e.

for the entire airplane, $\frac{1}{e} = \frac{1}{e_{wing}} + \frac{1}{e_{fuselage}} + \frac{1}{e_{other}}$ (3.44b)

Reference 3.6, section 3.2 recommends $\left(\frac{1}{e_{other}}\right)$ as 0.05.

3.2.17 Parabolic drag polar, parasite drag, induced drag and Oswald efficiency factor

It was mentioned earlier that the drag polar can be obtained by adding the drag coefficients of individual components at corresponding angles of attack. This procedure needs a large amount of detailed data about the airplane geometry and drag coefficients. A typical drag polar obtained by such a procedure or by experiments on a model of the airplane has the shape as shown in Fig.3.21a. When this curve is replotted as C_D vs C_L^2 (Fig.3.21b), it is found that over a wide range of C_L^2 the curve is a straight line and one could write:

$$C_D = C_{D0} + KC_L^2 \qquad (3.45)$$

C_{D0} is the intercept of this straight line and is called zero lift drag coefficient or parasite drag coefficient (Fig.3.21b).

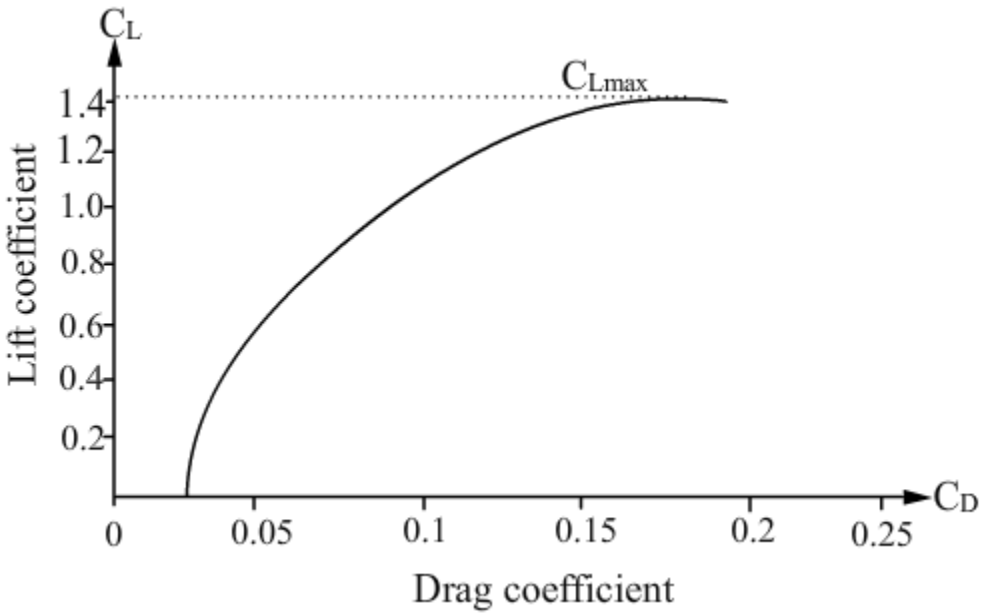

Fig.3.21a Typical drag polar of a piston – engined airplane

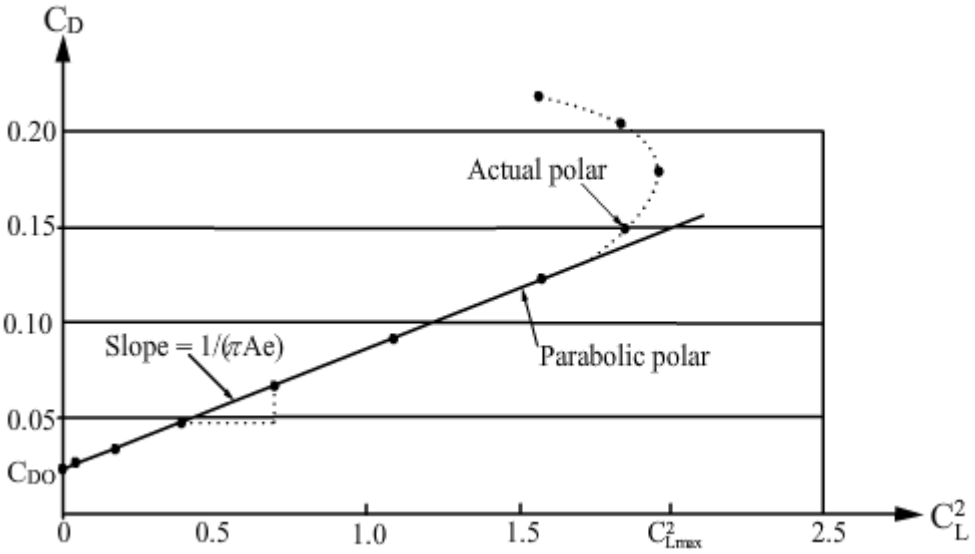

Fig.3.21b Drag polar replotted as C_D vrs. C_L^2

The term KC_L^2 is called induced drag coefficient or more appropriately lift dependent drag coefficient. K is written as:

$$K = \frac{1}{\pi A e} \tag{3.46}$$

The quantity 'e' in Eq.(3.46) is called 'Oswald efficiency factor'. It includes the changes in drag due to angle of attack of the wing, the fuselage and other components as expressed by Eq.(3.44b). It may be added that in the original definition of Oswald efficiency factor, only the contribution of the wing was included. However, the expression given by Eq.(3.44b) is commonly employed(Ref.1.12, Chapter 2 and Ref.3.6, Chapter 2).

The drag polar expressed by Eq.(3.45) is called 'Parabolic drag polar'.

Remarks:

i) A parabolic expression like Eq.(3.45) fits the drag polar because the major contributions to the lift dependent drag are from the wing and the fuselage and these contributions are proportional to the square of the angle of attack or C_L.

ii) **Rough estimate of C_{Do} :**

Based on the description in Ref.1.9, chapter 4 and Ref.3.7, chapter 14, the parasite drag ($D_{parasite}$ or D_0) of an airplane can be approximately estimated as the sum of the minimum drags of various components of the airplane plus the correction for the effect of interference.

Modifying Eq.(3.1), the parasite drag can be expressed as:

$$D_{parasite} = D_0 = (D_{min})_{wing} + (D_{min})_{fuse} + (D_{min})_{ht} + (D_{min})_{vt} + (D_{min})_{nac} + (D_{min})_{lg} + (D_{min})_{etc} + D_{int} \quad (3.46a)$$

Modifying Eq.(3.5), the above equation can be rewritten as :

$$D_0 = \frac{1}{2}\rho V_\infty^2 S (C_{Dmin})_{wing} + \frac{1}{2}\rho V_\infty^2 S_{fuse} (C_{Dmin})_{fuse} + \frac{1}{2}\rho V_\infty^2 S_{nac} (C_{Dmin})_{nac} + \frac{1}{2}\rho V_\infty^2 S_{ht} (C_{Dmin})_{ht} + \frac{1}{2}\rho V_\infty^2 S_{vt} (C_{Dmin})_{vt} + \frac{1}{2}\rho V_\infty^2 S_{lg} (C_{Dmin})_{lg} + \frac{1}{2}\rho V_\infty^2 S_{etc} (C_{Dmin})_{etc} + D_{int} \quad (3.46b)$$

Dividing Eq.(3.46b) by $\frac{1}{2}\rho V_\infty^2 S$ yields:

$$C_{D0} = (C_{Dmin})_{wing}\frac{S}{S} + (C_{Dmin})_{fuse}\frac{S_{fuse}}{S} + (C_{Dmin})_{nac}\frac{S_{nac}}{S} + (C_{Dmin})_{ht}\frac{S_{ht}}{S} + (C_{Dmin})_{vt}\frac{S_{vt}}{S} + (C_{Dmin})_{lg}\frac{S_{lg}}{S} + (C_{Dmin})_{etc}\frac{S_{etc}}{S} + C_{Dint} \quad (3.46c)$$

To simplify Eq.(3.46c) the minimum drag coefficient of each component is denoted by $C_{D\pi}$ and the area on which it is based is called 'Proper drag area' and denoted by S_{π}. Thus, when the contribution of fuselage to C_{Do} is implied, then $C_{D\pi}$ refers to $(C_{Dmin})_{fuse}$ and S_{π} refers to S_{fuse}. With these notations Eq.(3.46c) simplifies to :

$$C_{D0} = \left(\frac{1}{S}\sum C_{D\pi} S_{\pi}\right) + C_{Dint} \quad (3.46d)$$

The product $(C_{D0} S)$ is called 'Parasite drag area'.

Note :

1)See example 3.3 for estimation of C_{D0} of a low speed airplane.

2) In Appendices A and B the parasite drag coefficient (C_{D0}) is estimated using the procedure given in Ref.3.6, chapter 3, which in turn is based on Ref.3.5, section 4.5.3.1. In this procedure the contributions of the wing and fuselage to C_{D0} are estimated togather as wing – body combination and denoted by C_{D0WB}

iii) The parabolic polar is an approximation. It is inaccurate near $C_L = 0$ and $C_L = C_{Lmax}$ (Fig.3.21b). It should not be used beyond C_{Lmax}.